JJEES

Volume 6, Number 2, December, 2014
ISSN 1995-6681
Pages 67- 75

Jordan Journal of Earth and Environmental Sciences

Effect of Oil Shale Ash on Static Creep Performance of Asphalt-Paving Mixtures

Qahir N. Al-Qadi[1], Arabi N. Al-Qadi[2*], and Taiser S. Khedaywi[3]

[1] Department of Earth Sciences and Environment, the Hashemite University, Zarqa, Jordan.
[2] Corresponding Author: Department of Civil Engineering, AL Hussien Bin Talal University, Ma'an.
[3] Department of Civil Engineering, Jordan University of Science and Technology, Irbid, Jordan.

Received 2 May, 2014; Accepted 4 December, 2014

Abstract

The objectives of the present study are to evaluate the effect of oil shale ash on the rutting of flexible pavement and to find the optimum percentages of ash, which will give the best properties of flexible pavement. Oil shale ash was used as an additive in an asphalt concrete mix. Specimens, with five-ash content (0%, 5%, 10%, 15% and 20%) by volume of binder, were made by Marshall Moulds. Then they were exposed to creep tests (static) through the Universal Testing Machine (UTM). Three testing temperature levels (5°C, 25°C and 40°C) resembling relatively cold, moderate and high levels of temperature were considered. Oil shale ash is an air and water pollutant by product of oil shale rock. This research attempt to recycle oil shale ash by using it as an additive to hot mix asphalt (HMA). Furthermore, it will decrease the economic costs of constructing asphalt mix. The optimum percentage (12.5%) of oil shale ash addition it will increase the quality and performance of asphalt mix by reducing rutting. Statistical models analysis of the data provided by the UTM, consequently, this increased stiffness, resilient modulus and the accumulated strain of the asphalt concrete mix. Moreover, rutting depth and air voids were decreased.

Keywords: Static creep; Universal testing machine; Oil shale ash; Flexible pavement; Marshall Test.

1. Introduction

One of the Oil Shale rocks spreading in Jordan is the Sultani deposit located near Amman with 100 Km the south direction. The use of oil shale as a source of energy in Jordan will lead to environmental hazardous oil shale ash coming to the surface. Most of the forecast of the world energy demand agree that conventional energy resources are not sufficient to meet the energy requirement of an expanding world economy beyond the year 2020. (Ministry of energy and mineral resources, 1995); hence the need for benefiting from this ash in asphalt constructions.

This study will investigate methods that will help reducing the pollution of the environment in Jordan, when oil shale is used as a major source of energy in the future. In addition, oil shale ash, as an additive substance to asphalt cement pavement forming a binder; is available and of low cost. Characteristics of asphalt mixtures can be evaluated using conventional tests, such as Marshall and Hveem tests. In addition, many studies were undertaken to improve the properties of asphaltic concrete mixtures by additives.

Several studies (Van de loo, 1976 and1974) indicate that the conventional bituminous mixture tests cannot provide information about the rutting potential of paving mixtures. The use of oil shale ash in road construction materials, on the long run, focusing on static creep test, were investigated to demonstrate the effect of ash content on accumulated strain, stiffness, resilient modulus and rutting (permanent deformation) by using UTM.

Young-Chan *et al*. (2011) studied the Accelerated Pavement Testing (APT) with temperatures and air void ratio factors. These are the most important factors that influence rutting (permanent deformation). The purpose was to use APT results to calibrate and develop a laboratory rutting models for asphalt concrete mixtures. The layer of asphalt concrete tested was of 30cm, and sub-base 30cm, and sub-grade of 180cm, at temperature 50°C and air voids (7.31% to 10.57%) measurement of the plastic and resilient strain.

Gui-ping and Wing-gun (2007) investigated the effects of bitumen grade, the content of Reclaimed Asphalt Pavement (RAP) material and the aging of RAP. The study presents the evaluation of permanent deformation of Foamed Asphalt (FA) mixes by using the dynamic creep test. The mix design of WC-20 was conducted based on the graduation requirement of FA mix and RAP aggregate size. Three factors, namely Creep Strain Slope (CSS), Intercept, and Secant Creep Stiffness Modulus (SCSM), were used to analyze the test results. Mean comparison and multiple analyses of variance (ANOVA) reveal that bitumen grade significantly affects CSS, whilst content and aging of RAP would have an insignificant effect on CSS. High bitumen grade also helps FA mixes on the reduction of susceptibility to permanent deformation. Test results reflect that variances of CSS, Intercept, and SCSM are large and they also lead to the conclusion that there is a good exponential relationship between CSS and SCSM. However, no correlation between CSS and air void is found. The comparison between the test results of FA mixes and those of hot asphalt mixes exhibits that susceptibility and creep strength of FA mixes are better than those of the selected hot asphalt mixes.

Biligiri *et al.* (2007) studied several mathematical models to be used in calculating the onset of tertiary flow for asphalt

* Corresponding author. e-mail: arabi.alqadi@gmail.com

mixtures. The Flow Number (FN) indicates the onset of shear deformation in asphalt mixtures, which is a significant factor in evaluating rutting in the field. They found that the FN is obtained from the Repeated Load Permanent Deformation (RLPD) laboratory test. The current modelling techniques in determining the FN use a polynomial model fitting approach, which works well for most conventional asphalt mixtures. Biligiri *et al.* (2007) offered an analysis and some observations on the use of this polynomial model for rubber-modified asphalt mixtures, showing that the problems lie in identifying the true FN values. Their scope were to collect and analyze more than 300 RLPD test data files, which comprised more than 40 mixtures, a wide range of test temperatures, and several stress levels. A new comprehensive mathematical model was recommended to accurately determine the FN. The results and analyses were evaluated through manual calculations and they found them accurate, rational, and applicable to all mixture types.

Carpenter and Vavrik (1999) recognized the need for a simple test that can be preferably performed on a super pave gyratory compactor (SGC) samples during mix design that would rank the performance potential of the mixtures. They proved of the difficulties of finding one test that can rate mixture potential for rutting, fatigue cracking and modulus. They used Illinois mixtures that provide evidence that a simple test performed during mix design has the potential of predicting a diverse set of performance characteristics. Their results are presented for 10 Illinois dense-graded mixtures of surface and binder (9.5mm and 12.5mm) gradations that were tested in an Asphalt Pavement Analyzer (APA) and subjected to flexural beam fatigue, unconfined repeated load permanent deformation, and diametric resilient modulus testing. The mixtures were subjected to a rapid triaxial test procedure using SGC compacted samples, as taken from the SGC machine, and tested at 50^{o}C in a triaxial stress reversal mode. The triaxial testing provides data that predict resilient modulus, APA rutting results, fatigue coefficients, and permanent deformation characteristics of accumulated strain at tertiary failure, loads to tertiary failure, and the exponent to the standard logarithmic permanent deformation curve. The excellent correlations obtained from this study provide direct evidence that this test protocol may provide a structural evaluation procedure to supplement the volumetric mix design process.

Vacin *et al.* (1999) used samples of one polymer-modified asphalt mixing with fine filler (mastic), and one HMA prepared with the same modified asphalt as binders were tested in the Dynamic Ahear Rheometer (DSR) and the Bending Beam Rheometer (BBR). The materials were tested to characterize discrete relaxation and retardation spectra (under the condition of small deformations). DSR testing was performed in the plate–plate and the torsion bar geometry. From the obtained relaxation and retardation spectra, the shear compliance, J(t), was calculated and compared with the tensile creep compliance, D(t), measured in BBR. A simple relationship between J(t) and D(t) was found for the asphalt binder and the asphalt mastic. In the case of HMA, the bulk compliance, B(t), contributes to D(t) at short and long times. Both the Boltzmann superposition principle and the time–temperature superposition principle hold very well for all the tested materials at low temperatures. They conclude that there are qualitative differences in the rheological behaviour of the asphalt binder and the asphalt mastic on one side and the HMA on the other. These differences can be seen in dynamic (DSR) as well as in transient (BBR) experiments.

Abo-Qudais and Shatnawi (2007) tried to predict the number of the cycles causing a fracture in Hot Mix Asphalt (HMA) with the slope of accumulated strain turn from decreasing to increasing mode of failure. Furthermore, they studied the effect of aggregate gradation and temperature on the fatigue behaviour of HMA. They used Marshall Test to find the optimum asphalt content. The material they used were crushed lime stone, penetration of asphalt 60/70, and three gradation of aggregate with maximum nominal size of 12.5mm, 19mm, and 25mm; five magnitude of loading (1.5KN, 2.0KN, 2.5KN, 3.0KN, and 3.5KN) were studied. Temperatures 10^{o}C, 25^{o}C, 45^{o}C, and 60^{o}C were used to evaluate the load at 3.5KN. They concluded that the slope of accumulated strain decreases until the number of the cycles loading reach 44% of fracture cycles of HMA, and the stiffness increases as the applied load increases and the gradation maximum nominal size decreases.

Oil shale ash, as a by-product of oil shale burning, causes serious environmental problems; but using it in flexible pavement material decreases the cost of road constructions.

The present study aims at:

- investigating the feasibility of using oil shale ash as an additive to the asphalt bituminous paving mixtures to achieve economic advantage and good performance;
- determination the effect of oil shale ash on static creep of flexible pavement by studying the responses (stiffness, accumulated strain, and rutting) ; and
- finding the optimum percentage of ash, thus giving the best properties via reducing rutting and air voids

2. Approach of the Study

To achieve the objectives of this study, Hot Mix Asphalt (HMA) specimens were prepared at optimum asphalt content using Marshal mix design procedure (MS-2, 1976). Marshal compactor was used to compact the HMA specimens. Limestone aggregate, asphalt with 60/70 penetration, Oil shale were used as an additive to the asphalt cement composed of oil shale ash burned at 600^{o}C, which passed a #200 sieve, was tested as an additive to asphalt cement. In preparing ash-asphalt binders, ash and asphalt contents were heated and maintained at a temperature between 145^{o}C and 150^{o}C (293^{o}F and 302^{o}F) (Al-Massaid *et al*., 1989). Tests include the characteristics of the materials used in the research, preparation of binders, and optimum asphalt determination. Also, the present study presents a static creep test on asphalt-ash concrete specimens.

3. Materials Used

Aggregate

One type of aggregate was used in the study; it was brought from Al-Halabat quarries in Jordan. Gradation was according to the Ministry of Public Works and Housing (MPWH) specification in Jordan (1991). Table (1-A) shows the aggregate properties while Table (1-D) lists the aggregate gradation.

Asphalt

One penetration grade of asphalt cement (60–70) was used in this study. Asphalt was obtained from the Jordan Petroleum Refinery Company in Zarqa, Jordan, and it is widely used in flexible pavement constructions. Table 1-B summarizes the physical properties of the asphalt used in this study.

Table 1: A, B, C, D. Properties of the materials used in this study*

A. Aggregate Properties Used in Research				
Aggregate Type (Limestone)	ASTM Test Designation	Bulk Specific Gravity	Apparent Specific Gravity	Absorption (%)
Coarse Agg.	C127	2.426	2.618	3.0
Fine Agg.	C128	2.460	2.628	3.6
Mineral Filler	C128	2.485	2.485	5.0

B. Physical Properties of Asphalt		
Test	Methods	Results
Ductility, 25 ^{0}C,Cm	ASTM D 113	110
Penetration, 25 ^{0}C, 100 g, 5 s, 0.1 mm	ASTM D 5	65
Softening Point, ^{0}C	ASTM D 36	50
Flash Point (Cleveland Open Cup), ^{0}C Fire Point, ^{0}C	ASTM D 92 ASTMD92	330 335
Specific Gravity, 25 ^{0}C	ASTM D 70	1.014
C. Properties of Oil Shale Ash		
Properties	ASTM Designation	Test Result
Specific Gravity	C188	2.842
Color		Brown To Black
D. Aggregate Gradation Used		
Sieve Size	Specification Limits* (% Passing)	%Passing (Midpoint)
1» (25 mm)	100	100
¾» (19 mm)	90-100	95
½» (12.5 mm)	71-90	80.5
3/8» (9.5 mm)	56-80	68
No. 4 (4.75 mm)	35-56	45.5
No. 8 (2.35 mm)	23-38	30.5
No. 20 (850 µm)	13-27	20
No. 50 (300 µm)	5-17	11
No. 80 (180 µm)	4-14	9
No. 200 (75 µm)	2-8	5
*Ministry of Public Works and Housing (MPWH), Specification Sec. 4.01, Table 4.1 Wearing Mix (11)(1991).		

Oil Shale Ash

Oil shale was obtained from the Sultani deposit. Ash was produced by grinding the shale then burning it at 600^{o}C in an oven. It was then passed through a # 200 sieve to be used as an additive in the asphalt cement. The specific gravities of the binder (asphalt-ash) at 0%, 5%, 10%, 15%, and 20% by volume were 1.014, 1.089, 1.103, 1.216, and 1.325, respectively. Table 1-C presents the physical properties of the oil shale ash.

Determination of Optimum Asphalt Content for Conventional Mixes

To determine the optimum asphalt content by weight of total mixture, the procedure indicated by the standard Asphalt Institute MS-2 Manual (1976) and ASTM D1559 (1990) was determined using Marshal Mix design of 50 blow procedures (represent medium traffic). Three samples from each asphalt level (4.0%, 4.5%, 5.0%, 5.5%, and 6%) of the total weight of the mix were prepared. Specimens were extruded from the Marshall moulds after 24 hours. Height and weight measurements were conducted to determine the unit weight of each specimen, and specimens were submerged in water at 60^{o}C for 40 minutes before testing. A total of 15 specimens were tested for flow, stability, unit weight, air voids, and voids in mineral aggregate. The optimum asphalt content was measured as the average of asphalt contents that meet maximum stability, maximum unit weight, and 4.0% air voids; then the measured optimum asphalt contents were checked to figure out whether they are within the specification limits of the factors (flow, stability, air voids unit weight, and voids in mineral aggregate). The optimum asphalt content was found to be 5.4% by total weight of mixture.

4. Static Uniaxial Loading Strain Test

The method for the determination of resistance to permanent deformation of bituminous mixtures subject to unconfined uniaxial loading involves the application of a static load to a sample for 3600 second loading at different temperatures (5^{o}C, 25^{o}C, and 40^{o}C). It is performed by Universal Testing Machine (UTM). This test was conducted in accordance with UTM Reference Manual (1996) and BSI standards. The Marshall specimens with different percentages of ash (0%, 5%, 10%, 15%, and 20%) by volume of binder were tested using the UTM. Specimen heights with six measurements were taken and if the difference between the smallest and the largest of the six thickness measurements was more than 2% of the nominal diameter of the specimens, the specimen was levelled. Specimens were placed in a cabinet with a suitable force air circulation, in which the specimen gains the test temperature for 24 hour, and then the test was performed for different level of temperatures (5^{o}C, 25^{o}C, and 40^{o}C). Grease was spread evenly and thinly over the ends of the specimen to minimize friction. Surplus grease was removed with a cloth to leave surface with a damp appearance to minimize the friction at the platen-to-specimen interface.

Conditioning was made by the use of a software program in a stress of 10 KPa for 20 second. Specimen was subjected to static loading for 3600 second with a stress of 100 KPa. Then levelling was made in Linear Variable Displacement Transformers (LVDTs), data of accumulated strain, creep stiffness, slope of accumulated strain and temperature were measured by the assistance of a computer. Fig. 1 shows the testing setup.

Figure 1: Specimen in the static creep frame of a UTM.

5. Results and Discussion

5.1. Effect of Static Creep Test

Static creep test was developed to estimate the rutting potential of asphalt mixtures. This test was conducted by applying a static load to a HMA ash specimen and measuring the resulting permanent deformation with time. The most common creep test is the static unconfined. This test involves application of a static load to a sample for specified time and temperature and the measurement of deformation as the sample deforms (BSI, 1996).

Test of static uniaxial loading strain conforms to the requirements issued by the British Standards Institute (BSI part 111, 1995) for determination of resistance to permanent deformation of bituminous mixtures subjected to unconfined uniaxial loading. The tests initially apply conditioning stress to the specimen and measure the resulting accumulating strain. The magnitude and applied time duration of conditioning stress have present default values of 10 KPa and 120 second, and then the specimen was subjected to static loading for 3600 second with default s tress level of 100 KPa. During the full static loading stage, the accumulated strain is measured and displayed as a plot with linear scale axis.

Test proceeds; plotted data are displayed with linear vertical and horizontal axis. The output of this test is the selection of:

- accumulated strain (creep or permanent strain);
- derivative of accumulated strain (slope);
- applied stress;
- creep stiffness (modulus); and
- core temperature of a dummy specimen.

Static creep test was performed in order to obtain the accumulated strain, mix stiffness, creep compliance, and permanent deformation (rutting) for different oil shale ash contents. The recorded deformation, as a function of time of loading, was used to calculate accumulated strain, stiffness, and permanent deformation at three levels of temperature 5°C, 25°C, and 40°C.

5.2. Accumulated Strain

Accumulated strain is the ratio of the total deformation to the original height of the specimen at any instant of time during the test. Axial micro-strain was calculated according to the following formula in Eq. (1):

$$\epsilon ct = (L2t - L1)/G \qquad (1)$$

ϵct = is the accumulated axial strain (creep) at time t

L1 = is the initial zero reference displacement of the transducers before the full loading stress is applied.

L2t = the displacement level of the transducers at time t.

G = is the initial specimen length.

The axial micro-strain was calculated for different temperature levels (5°C, 25°C, and 40°C) and different oil shale ash content with the same asphalt content. The axial micro-strain was calculated for different temperature levels (5°C, 25°C, and 40°C) and different oil shale ash content with the same asphalt content (UTM 2 Manual, 1996). The relationship between accumulated strain and time at different temperature levels and percent of oil shale ash are shown in Fig. 2. Accumulated micro-strain versus time for (a) 0%, (b) 5%, (c) 10%, (d) 15%, and (e) 20% oil shale ash at different temperatures levels. This figure shows that there is a decrease in axial strain at low temperature, while at high temperature there is a certain increase.

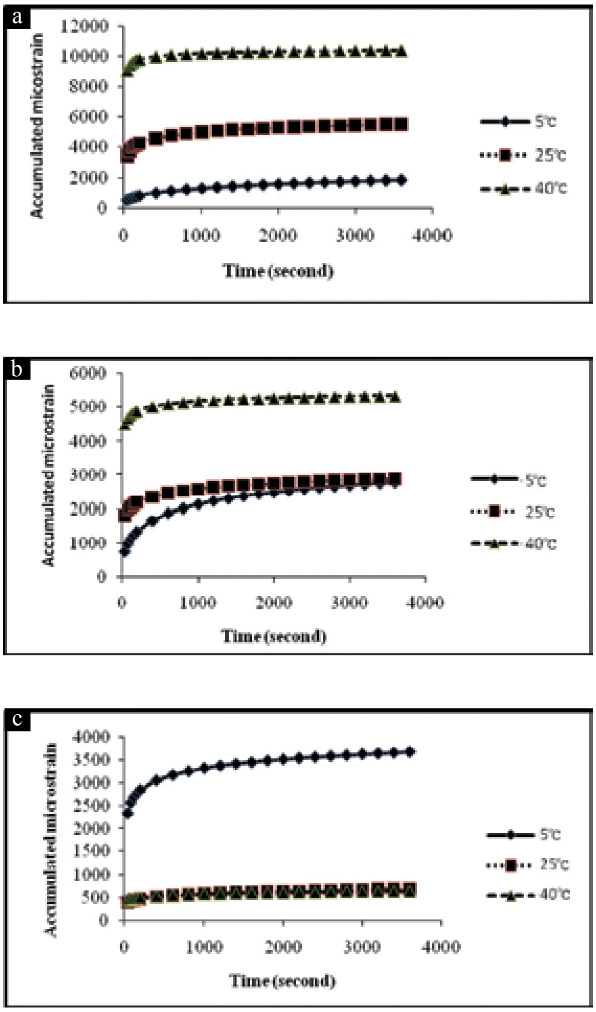

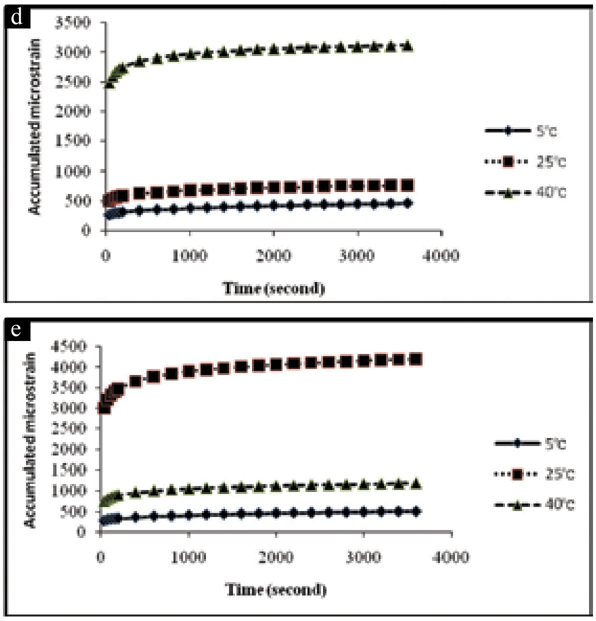

Figure 2: Accumulated micro-strain versus time for (a) 0 %, (b) 5%, (c) 10%, (d) 15%, and (e) 20% of oil shale ash at different temperature levels.

In Fig. 3 accumulated micro-strains versus time for different % of oil shale ashes contents at (a) 5°C, (b) 25°C, and (c) 40°C are shown, in a logarithmic scale, that as ash content increases the axial micro strain decreases; this is due to the fact that the adhesive forces between particles become relatively weak.

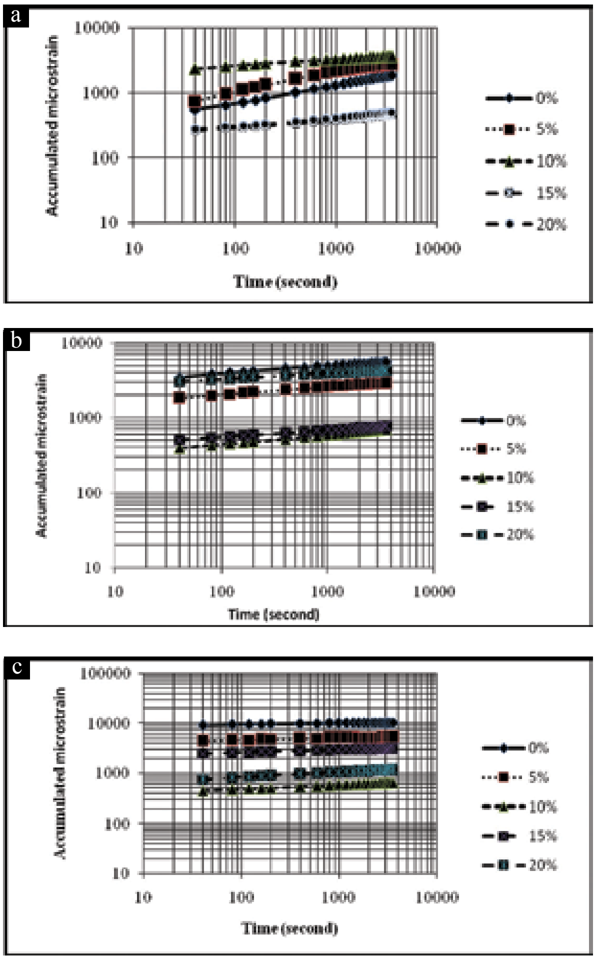

Figure 3: Accumulated micro-strains versus time for different % of oil shale ash content at (a) 5°C, (b) 25°C, and (c) 40°C.

5.3. Creep Stiffness

Stiffness (S_{mix}) is defined as the ratio of applied constant load to deformation as a function of time and temperature. Stiffness was calculated according to the following Eq. (2):

$$S_{mix} = \sigma/\epsilon s(t,T) \quad (2)$$

where

S_{mix} = is the static load stiffness modulus of the mixture at loading time t (in second) and loading temperature T (in °C).

ϵs = Static strain

σ = is the applied stress (in KPa).

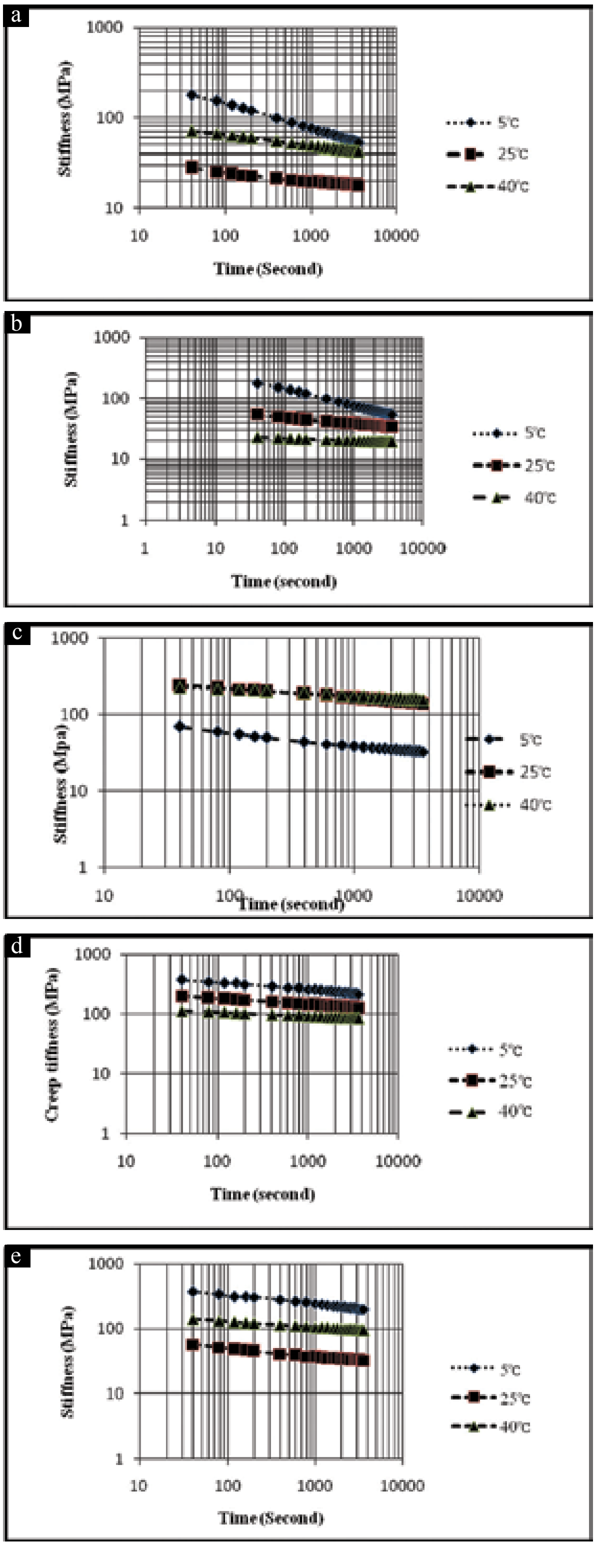

Figure 4: Creep stiffness versus time for (a) 0%, (b) 5%, (c) 10%, (d) 15%, (e) 20% of oil shale ash at different temperatures.

The stiffness values were calculated for different temperature levels and ash contents. Fig. 4 shows the creep stiffness versus time for (a) 0%, (b) 5%, (c)10%, (d) 15%, (e) 20% oil shale ashes at different temperatures, and Figs. 4(a) through (e) show the relationship between stiffness (S_{mix}) and time at different temperature and oil shale ash contents. As observed from the Figs. 4 (a-e), the highest stiffness in 0%, 5%, 15%, and 20% ash are seen at 5°C curve, and the lowest stiffness at 25°C for Figs. 4(a), and (e), and at 40°C in Figs. 4(b) and (d). In Fig. 4(c) the stiffness is high in 10% ash at 25°C and 40°C while it is low at 5°C. This implies that the 10% ash fraction can stand better than the other fraction in different climatic conditions, moderate and high temperatures; these are the ideal percentages; in fact this is the optimum.

At different ash content, stiffness versus time at different temperature, as shown in Figs. 5(a), (b), and (c), the stiffness decreases with the decrease in ash contents, while stiffness modulus for different ash content at different temperature 5°C, Fig. 5(a), the highest stiffness was seen in 20% and 0% and the lowest in 10% ash. In Fig. 5 (b), at 25°C the highest stiffness was observed in 10% and 15%, while the lowest at 0% ash. Also, in Fig. 5(c) at 40°C, the highest stiffness modulus at 10% ash was seen and the lowest in 5% ash.

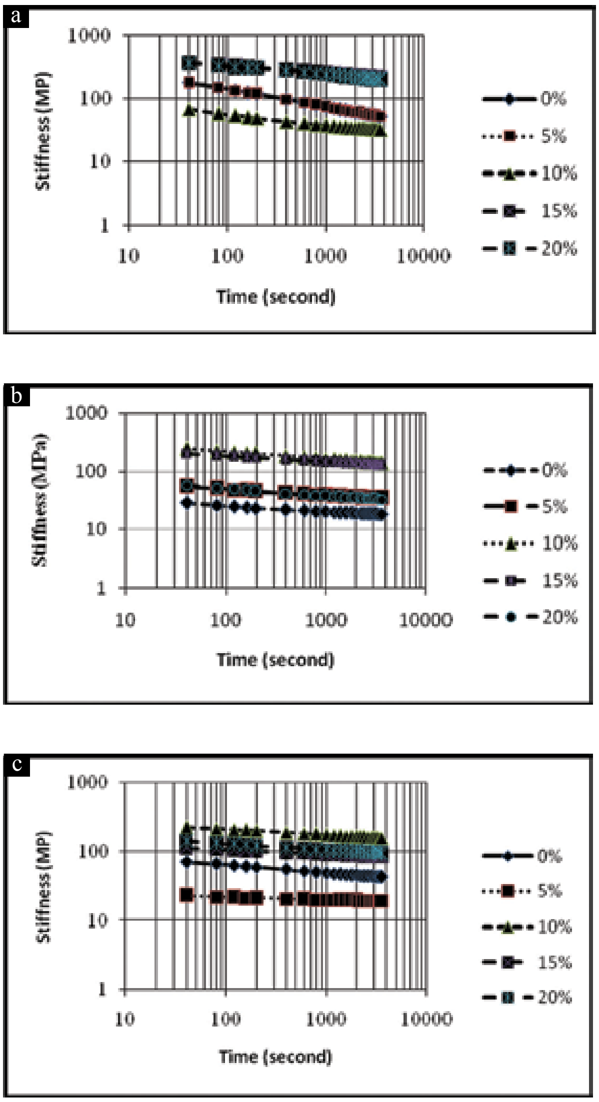

Figure 5: Stiffness versus time for different % of ash contents at (a) 5°C, (b) 25 °C, and (c) 40 °C.

6. Statistical Models for Air Voids, Stiffness Modulus and Accumulated Strain

To achieve the objectives of this study, 60 specimens were prepared for one type of aggregate (Limestone) with five levels of oil shale ash content. Static creep was carried out at three temperature levels. Graphical and statistical approaches were followed to investigate the effect of the oil shale ash additive on accumulated strain, stiffness, and air voids.

Tables 2, 3 and 4 contain a more realistic data set; the *X* represents the percentages of volume fraction (0%, 5%, 10%, 15% , and 20%) of oil shale ash in flexible pavement mixture, and *Y* represents the measured accumulated micro-strain and stiffness modulus at different temperatures (5°C, 25°C, and 40°C). These points do not clearly fall along a fitted line. These lines are shown in Figs. 5, 6 and 7 which provide a good fit to the data. The quadratic model assumes that the dependent or response variable, represented by Y_1 at 5°C, Y_2 at 25°C, and Y_3 at 40°C , are related to an independent variables, represented by *X*, by the relation as shown in the pure quadratic formula (3):

$$Y = \beta_o + \sum_{i=1}^{K} \beta_o \chi_i + \sum_{i=1}^{K} \beta_i \chi_i^2 + \Xi \qquad (3)$$

Where *Y* represents response variable, *βo* is the interception coefficient, *βi*, coefficient of the linear effect, and *βii*, the coefficient of quadratic effect. Where y represents an accumulated strain, and stiffness modulus for the pure quadratic model. The error term, Ξ is a normally distributed random variable with mean equal to 0.0 and standard deviation equal to σ. The error sum of square (SSE) was measured by the sum of squaring the residuals. A residual is a measure of the deviation of the data from the predicted or estimated regression line. SSE equal to 0.0 if all the data fitted perfectly in the line of regression and this indication for checking the data as the SSE increase means that the data more variable from the fitted line. The total sum of squares (SST) reveals, after the estimation of the mean number of accumulated strain, air voids and stiffness modulus at different percentages of oil shale ash, which percent is the optimum; our best estimate is the mean of micro-strain, air voids (%), and stiffness (MPa) by % of ash. The accuracy of the estimate is related to the variation of *Y* values around the mean. The sum of square about the mean is called the total sum of squares (SST).

Regression sum of squares (SSR) is when there is still some unexplained variation about the regression line. This implies that the regression line demonstrates an amount of variation equal to SST-SSE.

Coefficient of determination (R^2) is when all the data fall perfectly on a regression line, SSE=0.0, and SST=SSR. The value of R^2 is equal to 1.0. When there is no explanation for the variation of *Y*, SSR=0.0 then the R^2=0.0. When R^2 is expressed in percentages, it is related to SST which can be explained via using the predicted regression equation.

As seen in Figs. 6 through 8 and Tables 2, 3 and 4, the values of R^2 are equal to 0.999, 0.996, and 1.0 at 5°C, 25°C, and 40°C for measuring air voids, 0.996, 0.979, and 0.969 for stiffness modulus and 1.0, 0.999, and 0.999 for accumulated strain with a good fitness for representing the data. Also, the standard deviation of the errors for air voids equal to 0.0096, 0.122, and 0.176, stiffness modulus are 2.22, 6.15, and 1.91, and accumulated strain 2.58, 28.87, and 133.68 at 5°C, 25°C, and 40°C. These show that the lowest standard deviations of errors are cited at 5°C and in measurement of air voids (*Av*) with volume fraction of the oil shale ash percentages (*Vf*).

Table 2: Comparison of predicted, effectiveness and measured values and errors air voids of asphalt pavement mixtures with and without ash percents

Ash (%)	Air voids (%)											
	Measured			Predicted			Residual			Error Sum of Square(SSE)		
	5°C	25°C	40°C	5°C	25°C	40°C	5°C	25°C	40°C	5°C	25°C	40°C
0	4.8	4.1	3.5	4.811	4.034	3.762	-0.011	0.066	-0.262	0.000121	0.004356	0.068644
5	7.55	7.02	6.7	7.546	7.059	6.687	0.004	-0.039	0.013	1.6E-05	0.001521	0.000169
10	8.57	8.1	7.8	8.581	8.234	7.762	-0.011	-0.134	0.038	0.000121	0.017956	0.001444
15	7.92	7.7	7.1	7.916	7.559	6.987	0.004	0.141	0.113	1.6E-05	0.019881	0.012769
20	5.55	5	4.46	5.551	5.034	4.362	-0.001	-0.034	0.098	1E-06	0.001156	0.009604
	Measured-Mean			Predicted-Mean			Residual Error (%)*			Air void- Effectiveness (%)		
0	4.32	5.22	5.82	4.32	5.17	5.73	-0.23	1.64	-6.96	-	-	-
5	0.45	0.40	0.62	0.45	0.36	0.53	0.05	-0.55	0.19	57.29	70.73	91.43
10	2.86	2.94	3.56	2.86	2.90	3.47	-0.13	-1.63	0.49	78.54	97.56	122.85
15	1.086	1.73	1.41	1.09	1.69	1.32	0.051	1.87	1.62	65.00	87.80	102.85
20	1.764	1.92	2.11	1.76	1.87	2.02	-0.02	-0.68	2.25	15.63	21.95	31.43
	Total Sum of Square(SST)			Regression Sum of Square (SSR)			Coefficient of Determination (R^2)			Standard deviation of errors(S)		
	10.482	12.213	13.523	10.482	12.168	-119.48	0.999	0.996	1.0	0.0096	0.122	0.176

* Residual error (%) = ((measured value- residual value) / (residual value)) x100%

Table 3: Comparison of predicted, effectiveness and measured values and errors for stiffness modulus of asphalt pavement mixtures with and without ash percents of asphalt.

Ash (%)	Stiffness modulus (MPa)											
	Measured			Predicted			Residual			Error Sum of Square(SSE)		
	5°C	25°C	40°C	5°C	25°C	40°C	5°C	25°C	40°C	5°C	25°C	40°C
0	50	27	17	49	24.4	15.88	1	2.6	1.12	1.00	6.76	1.254
5	98	76	60	100.8	80.2	62.43	-2.8	-4.2	-2.43	7.84	17.64	5.905
10	129	107	90	126.6	110	89.28	2.4	-3	0.72	5.76	9.00	0.518
15	126	122	98	126.4	113.8	96.43	-0.4	8.2	1.57	0.16	67.24	2.465
20	100	88	83	100.2	91.6	83.88	-0.2	-3.6	-0.88	0.04	12.96	0.774
	Measured-Mean			Predicted-Mean			Residual Error (%)*			Stiffness- Effectiveness (%)		
0	2560.36	3249	2766.76	2545.56	3135.4	2755.843	2.04	10.66	7.05	-	-	-
5	6.76	64	92.16	-8.04	-49.6	81.243	-2.78	-5.24	-3.89	96	181	253
10	806.56	529	416.16	791.76	415.4	405.243	1.90	-2.73	0.81	158	296	429
15	645.16	1444	806.56	630.36	1330.4	795.643	-0.32	7.21	1.63	152	352	476
20	0.36	16	179.56	-14.44	-97.6	168.643	-0.20	-3.93	-1.05	100	226	388
	Total Sum of Square(SST)			Regression Sum of Square (SSR)			Coefficient of Determination (R^2)			Standard deviation of errors(S)		
	4019.2	5302	4261.2	4004.4	5188.4	4128.2	0.996	0.979	0.969	2.22	6.15	1.91

* Residual error (%) = ((measured value- residual value) / (residual value)) x100%

Table 4: Comparison of predicted, effectiveness and measured values and errors for accumulated strain pavement mixtures with and without ash percents.

Ash (%)	Accumulated micro-strain											
	Measured			Predicted			Residual			Error Sum of Square(SSE)		
	5°C	25°C	40°C	5°C	25°C	40°C	5°C	25°C	40°C	5°C	25°C	40°C
0	4081.9	5540	10412	4085	5551	10335	-3.1	-11	77	9.61	121	5929
5	2384.9	2894	6106	2382.4	2859	6288	2.55	35	-182	6.50	1225	33124
10	1175	1170	3587	1176.4	1203	3491	-1.4	-33	96	1.96	1089	9216
15	468.1	591	2000	467.2	583	1944	0.95	8.0	56	0.90	64	3136
20	255.6	1000	1600	254.6	999	1647	1.0	1.0	-47	1	1	2209
	Measured-Mean			Predicted-Mean			Residual Error (%)*			Accumulated strain- Effectiveness (%)		
0	5802317	10896601	32160241	5802297	10894101	32106627	-0.076	-0.198	0.745	-	-	-
5	506659.2	429025	1863225	506639.3	426525	1809611	0.107	1.224	-2.894	-41.57	-47.76	-41.36
10	248103.6	1142761	1331716	248083.6	1140261	1278102	-0.119	-2.743	2.750	-71.21	-78.88	-65.55
15	1452025	2715904	7513081	1452005	2713404	7459467	0.203	1.372	2.881	-88.53	-89.33	-80.79
20	2009306	1535121	9865881	2009286	1532621	9812267	0.393	0.100	-2.854	-93.74	-81.95	-84.63
	Total Sum of Square(SST)			Regression Sum of Square (SSR)			Coefficient of Determination (R^2)			Standard deviation of errors(S)		
	10018412	16719412	52734144	10018392	16716912	52734011	1.0	0.999	0.999	2.58	28.87	133.68

* Residual error (%) = ((measured value- residual value) / (residual value)) x100%

6.1 Air Voids Models

The improvements, as the air voids in Fig. 6 and Table 2, were 57.29, 70.73, and 91.43 for 5, 25, 40°C at 5% fraction; 78.54, 97.56, and 122.85 for 5°C, 25°C, and 40°C at 10% fraction, 65, 87, and 102.85 for 5°C, 25°C, and 40°C at 15 fraction, and reduced to 15.63, 21.95, and 31.43 at 20% fraction, being a reduction small compared to the maximum improvement at 10% fraction. The air voids improvement of fixable pavement mixture ranged from 57.29 to 78.54 for 5°C, 70.73 to 97.56, at 25°C, and 91.43 to 122.85 for 40°C to 20% fraction. The predicted models for air voids are as presented in Eqs. (4), (5), and (6):

$$Av=4.070+ 0.776\ Vf -0.036\ Vf^2 \quad (4)$$

$$Av = 3.522+ 0.816\ Vf -0.038\ Vf^2 \quad (5)$$

$$Av =4.802 + 0.718\ Vf -0.034\ Vf^2 \quad (6)$$

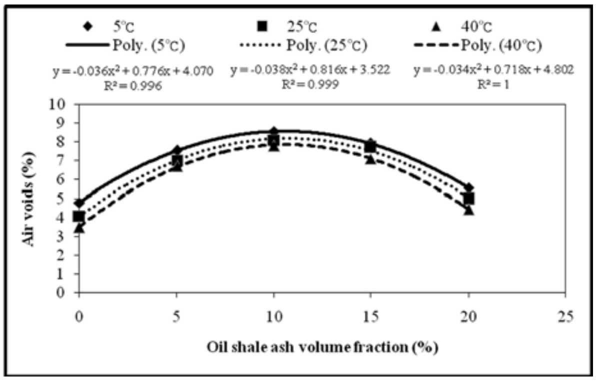

Figure 6: Effect of oil shale ash volume on air voids of asphalt pavement mixtures.

The air voids prediction using the above equations agreed favourably with the test results, as shown in Table 2. The production error runs below are 0.13%, 1.63%, and 6.96% at 5°C, 25°C, and 40°C, respectively.

6.2 Stiffness Modulus Models

The improvements, as the stiffness modulus in Fig. 7 and Table 3, were 96, 181, and 253 for 5% fraction, 158, 296, and 429 for 10% fraction, 152, 352, and 476 for 15% fraction, and 100, 226, and 388 for 20% fraction at 5°C, 25°C, and 40°C temperatures, and reduced at 20% fraction, being a reduction small compared to the maximum improvement at 15% fraction. The stiffness modulus improvements of fixable pavement mixture ranged from 96 to 158 for 5°C, 181 to 352, at 25°C, and 253 to 476 for 40°C to 20% fraction. The regression models of the stiffness modulus(Sm) are measured as seen in Eqs. (7), (8), and (9):

$$Sm =49+ 12.96\ Vf -0.52\ Vf^2 \quad (7)$$

$$Sm = 24.4+ 13.76\ Vf -0.52\ Vf^2 \quad (8)$$

$$Sm =15.88+ 11.28\ Vf -0.394\ Vf^2 \quad (9)$$

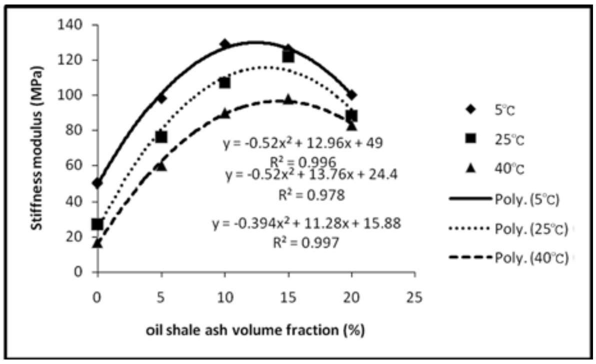

Figure 7: Effect of oil shale ash volume on stiffness modulus of asphalt pavement mixtures.

The air voids prediction using the above equations agreed favourably with the test results, as shown in Table 3. The production error runs below are 2.78%, 5.24%, and 3.89% at 5°C, 25°C, and 40°C, respectively.

6.3 Accumulated Strain Models

The reductions as the accumulated strain in Fig. 8 and Table 4 were 41.57, 47.76 and 41.36 for 5% fraction71.21, 78.88, and 65.55 for 10% fraction, 88.53, 89.33, and 80.79 for 15% fraction, and 93.74, 81.95, and 84.63 for 20% fraction at 5°C, 25°C, and 40°C temperatures, and increase at 20% fraction, being a reduction small compared to the maximum improvement at 5% fraction. The accumulated strain reduction of fixable pavement mixture ranged from 41.57 to 93.74 for 5°C, 47.76 to 81.95, at 25°C, and 41.36 to 84.63 for 40°C to 20% fraction. Models of accumulated strain (As) are shown below in Eqs. (10), (11), and (12):

$$As = 4085- 390.2\ Vf +9.934\ Vf^2 \quad (10)$$

$$As =5552- 642.3\ Vf + 20.73\ Vf^2 \quad (11)$$

$$As =10336- 934.2\ Vf +24.98\ Vf^2 \quad (12)$$

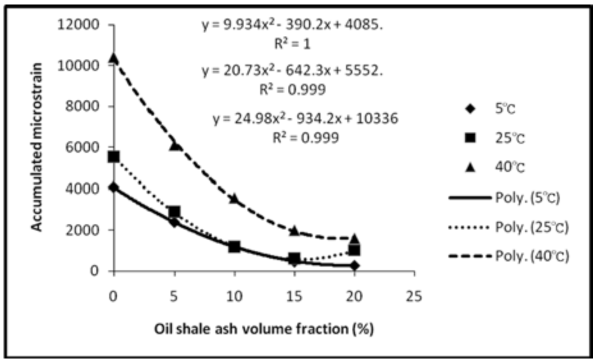

Figure 8: Effect of oil shale ash volume on accumulated strain of asphalt pavement mixtures.

The air voids prediction using the above equations agreed favourably with the test results, as shown in Table 4. The production error runs below are 0.119%, 2.743%, and 2.854% at 5, 25, and 40°C, respectively.

7. Conclusions

The following conclusions were drawn:

- The addition of a certain percentage of oil shale ash (10 – 15%) improves the stiffness of bituminous mixtures because it increases the adhesive forces between the asphalt and the aggregate. Thus, the mechanical interlocking between the aggregate particles is improved by this treatment.
- Temperature has a significant effect on resilient modulus and creep stiffness, so as temperature decreases, resilient and stiffness modulus increase. Accumulated strain increases if the oil shale ash is within the optimum, then decreases with the increase in oil shale ash content above the optimum.
- Stiffness decreases with time for different oil shale ash contents at different levels of temperature. Maximum stiffness was found at 5oC and ash was at 10%.
- The predictive model is statistically significant with a coefficient of multiple determinations R2 of 0.715; also, the model and the included variables had a high level of significance (0.002); there is a decrease in the rutting potential of the asphaltic-ash mixtures as the amount of ash increases.

Acknowledgment

Authors sincerely thank The Founder Professor of Engineering Imad L. AL-Qadi, PhD, PE, Dist. M. ASCE, Illinois Center for Transportation, Director, Advanced Transportation Research and Engineering Lab, Director, for his constructive encouragement and support to carry this experimental investigation.

References

[1] Al-Massaid, H., Taiser Khedaywi, and Mohammed Smadi. 1989. Properties of Asphalt-Oil Shale Ash Bituminous Mixtures under Normal and Freeze-Thaw Condition. Transportation Research Record (TRB), National Research Council, Washington, D.C, Vol. 1228, PP.54-62.

[2] Annual Book of ASTM Standards, (ASTM D1559) 1990. Road and paving materials. Vol.4.03, pp. 206-211.

[3] Biligiri Krishna P., Kaloush Kamil E., Mamlouk Michael S., and Witczak Matthew W., 2007. Rational Modeling of Tertiary Flow for Asphalt Mixtures. Transportation Research Record: Journal of the Transportation Research Board, No. 2001, Transportation Research Board of the National Academies, Washington, D.C., pp. 63–72. DOI: 10.3141/2001-08.

[4] Carpenter Samuel H. and William R. Vavrik,1999. Repeated Triaxial Testing During Mix Design for Performance Characterization", Transportation Research Record 1767, Paper No. 01-3219, Paper No. 01-3219

[5] Gui-ping He a,b, Wong Wing-gun, 2007. Laboratory study on permanent deformation of foamed asphalt mix incorporating reclaimed asphalt pavement materials. Construction and Building Materials, Vol. 21, PP.1809–1819.

[6] Khashayer Hadipour and Kenneth O. Anderson. 1972. An Evaluation of Permanent Deformation and Low Temperature Characteristics of Some Recycled Asphalt Concrete Mixtures. Association of Asphalt Paving Technologists, PP. 615-644.

[7] Krishna P. Biligiri, Kamil E. Kaloush, Michael S. Mamlouk, and Matthew W. Witczak, 2007. Rational Modeling of Tertiary Flow for Asphalt Mixtures. Transportation Research Record: Journal of the Transportation Research Board,No. 2001, Transportation Research Board of the National Academies, Washington, D.C., pp. 63–72. DOI: 10.3141/2001-08.

[8] Method for Determination of Resistance to Permanent Deformation of Bituminous Mixtures Subject to Unconfined Universal Loading (BSI), 1995. BSI, Part111, PP. 1-8.

[9] Method for Determining Resistance to Permanent Deformation of Bituminous Mixtures Subject to Unconfined Dynamic Loading. 1996. DD226, PP. 1-6.

[10] Ministry of Energy & Mineral Resources., 1995. Natural Resources Authority (Basic Information on Oil Shale in Jordan), Amman-Jordan, Feb., pp 3-13.

[11] Ministry of Public Works & Housing Directorate of Planning & Development Specification. 1991. Highway and Bridge Construction., Sec. 4.01, Table 4.1, Amman, PP.4-5.

[12] Mix Design Method for Asphalt Concrete and Other Hot Mix Types. 1976. Asphalt Institute, MS-2, PP. 17-32.

[13] Saad Abo-Qudais and Ibrahem Shatnawi., 2007. "Prediction of bituminous mixture fatigue life based on accumulated strain", Construction and building Materials, Vol. 21, PP. 1370-1376.

[14] Universal Testing Machine (UTM) 2 Manual, 1996.Test no: 036. Static Uniaxial Loading Strain Test. K B de Vos, Oct.-99. BSI, PP.1-23.

[15] Vacin Ota J., Stastna Jiri, and Zanzotto Ludo, 1999. Creep Compliance of Polymer-Modified Asphalt, Asphalt Mastic, and Hot-Mix Asphalt. Transportation Research Record 1829, Paper No. 03-3152.

[16] Van de Loo P. J., 1974. Creep Testing, A Simple Tool to Judge Asphalt Mix Stability. Association of Asphalt Paving Technologists (AAPT), PP. 253-284.

[17] Van de Loo P. J., 1976. Practical Approach to the Prediction of Rutting in Asphalt Pavements: The Shell Method. Koninklijke / Shell-Laboratorium, Anesterdam,pp.15-21.

[18] Young-Chan Suh, Nam-Hyun Cho, Sungho Mun, 2011. "Development of mechanistic–empirical design method for an asphalt pavement rutting model using APT.", Construction and Building Materials, Vol.25, pp. 1685–1690.